Bioorganic Chemistry 54 (2014) 7–11

Contents lists available at ScienceDirect

Bioorganic Chemistry

journal homepage: www.elsevier.com/locate/bioorg

Template-directed synthesis of a small molecule-antisense conjugate targeting an mRNA structure

Yang Liu, Lilia Rodriguez, Michael S. Wolfe *

Center for Neurologic Diseases, Harvard Medical School, Brigham and Women's Hospital, Boston, MA 02115, United States

ARTICLE INFO

Article history:
Received 19 November 2013
Available online 13 March 2014

Keywords:
Tau
mRNA splicing
RNA hairpin
Click chemistry

ABSTRACT

The targeting of structural features in mRNA with specificity remains a great chemical challenge. A hairpin structure near exon 10 in the pre-mRNA encoding the tau protein controls its splicing, and dementia-causing mutations that disrupt this structure increase exon 10 splicing. We previously reported the discovery of small molecules, mitoxantrone (MTX) and analogs, which bind to the tau RNA hairpin structure and the design of bipartite antisense oligonucleotides (ASOs) that simultaneously bind to the discontinuous sequences that flank this hairpin. Herein we report the synthesis of a bipartite ASO conjugated to MTX using the tau RNA hairpin and flanking sequences as a template. A set of six MTX analogs, each containing a linker-azide, and a set of ten bipartite ASOs, each containing a branched linker-alkyne, were synthesized and tested in combinatorial fashion for their ability to conjugate in the presence or absence of template RNA. A single template-dependent MTX–ASO conjugate was identified from among the 60 reaction mixtures, demonstrating that the MTX and ASO precursors could simultaneously bind the RNA template and allow proper positioning of azide and alkyne for 1,3-cycloaddition. While the MTX–ASO conjugate proved too cytotoxic for cell-based assays, the conjugate inhibited tau exon 10 splicing under cell-free conditions more effectively than MTX or bipartite ASO alone.

1. Introduction

Structural motifs within mRNA, such as hairpins, G-quadruplexes, and riboswitches, can control various aspects of mRNA biology, including exon splicing, protein translation, and degradation [1–4]. As these structures regulate mRNA function, they may be worthwhile targets for ligand design [5–7]. Our focus has been on a structural motif that controls the alternative splicing of pre-mRNA encoding the microtubule-associated protein tau. Pathological tau filaments are a common feature of a variety of neurodegenerative brain disorders [8], and rare dominant mutations in the tau gene cause familial forms of dementia [9–11]. Many of these mutations are silent, only increasing the splicing of exon 10. Thus, altered tau pre-mRNA splicing to increase isoforms that include exon 10 is sufficient for tau pathology, neurodegeneration and dementia. The disease-causing mutations that shift splicing are found in and around a hairpin structure at the boundary between exon 10 and intron 10 (Fig. 1a) [12,13]. The disruption of this hairpin allows access to splicing factors that then increase exon 10 inclusion, while hairpin stabilization via artificial mutations have the opposite effect [14].

For these reasons, compounds that bind and stabilize the hairpin structure should decrease exon 10 splicing and counteract the effects of the dementia-causing mutations. We previously reported a high-throughput screen to identify small, organic molecules that bind and stabilize the tau RNA hairpin and discovered mitoxantrone (MTX) as such a ligand [15]. Elucidation of the structure of MTX bound to the tau RNA hairpin by NMR revealed that the anthracene-dione ring system intercalates between two G–C base pairs, adjacent to an unpaired adenosine and close to the base of the hairpin (Fig. 1a), with the two N-(2-aminoethyl)ethanolamine substituents residing along the major groove [16]. Synthesis and evaluation of MTX analogs validated this structural model and led to the discovery that adding a third or fourth N-(2-aminoethyl)ethanolamine substituent to the other side of the anthracene-dione ring system (MTX-3 and MTX-4, respectively) is compatible with binding and stabilization of the tau RNA hairpin [17]. However, MTX and its analogs did not display specificity for

Abbreviations: ABU, linker alkyne building unit; ASO, antisense oligonucleotide; EGL, ethylene glycol-containing linker unit; MTX, mitoxantrone; PNA, peptide nucleic acid.

* Corresponding author. Address: Center for Neurologic Diseases, Brigham and Women's Hospital, 77 Avenue Louis Pasteur, H.I.M. 754, Boston, MA 20115, United States. Fax: +1 617 525 5252.

E-mail address: mswolfe@partners.org (M.S. Wolfe).

http://dx.doi.org/10.1016/j.bioorg.2014.03.001
0045-2068/

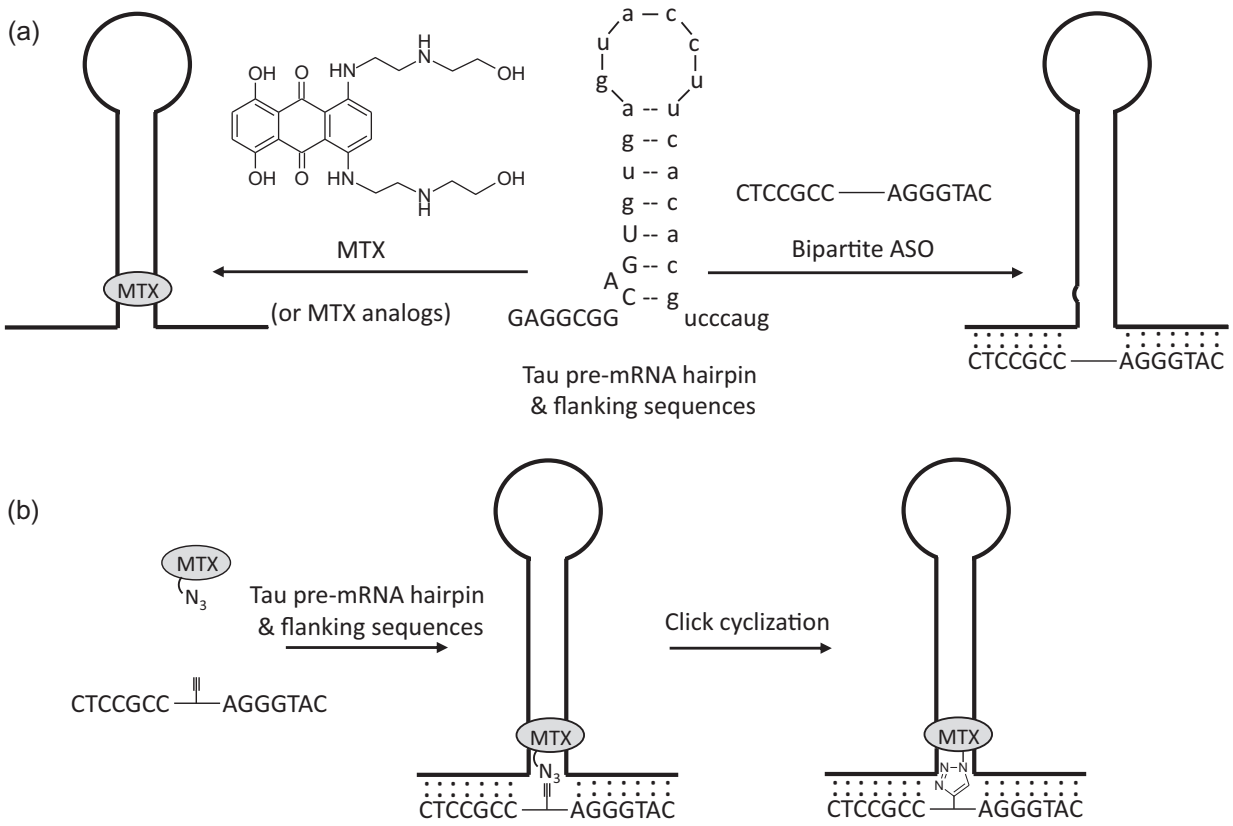

Fig. 1. (a) Tau pre-mRNA hairpin and flanking sequences and sites of binding by MTX and (left) and bipartite ASOs (right). Tau RNA exonic sequence in upper case, and intronic sequence in lower case. (b) Strategy for template-directed synthesis of MTX-ASO conjugates.

the tau RNA hairpin over other RNA hairpins, and even with a model of the bound structure, the design of more specific analogs was not obvious.

Our efforts then turned to the design of bipartite antisense oligonucleotides (ASOs) that would simultaneously bind the 5′ and 3′ sequences that flank the tau RNA hairpin, keeping the hairpin closed by virtue of a linker connecting the two antisense components. We envisioned the bipartite ASOs would bind to the tau RNA so that the linker region would be close to the MTX binding site at the base of the hairpin (Fig. 1a), with the possibility of ultimately conjugating MTX to the bipartite ASO for improved potency and specificity. Upon demonstrating the ability of the bipartite ASOs to inhibit tau exon 10 splicing, both under cell-free conditions and in whole cells [18], we sought a means to identify tripartite compounds: bipartite ASOs conjugated to MTX or its analogs. Herein we describe a template-directed approach to such MTX–ASO conjugates, screening a variety of MTX analogs and ASOs in a combinatorial manner for their ability to join via azide–alkyne Hüisgen cycloaddition (“click chemistry”) in the presence of tau RNA oligonucleotide template (depicted schematically in Fig. 1b).

2. Results and discussion

2.1. Strategy and design

Although we had an NMR-based model for how MTX is bound to the tau RNA hairpin, it was still unclear what would be the optimal design of an MTX–ASO conjugate in terms of (1) linker length between MTX and ASO, (2) placement of the linker on MTX, (3) the exact sequence of the ASO, (4) the conformational flexibility of the branched linker in the bipartite ASO, and (5) the location of the branch in the ASO linker region. For these reasons, a template-directed strategy promised particular efficiency, allowing the target RNA structure and flanking sequences to guide us to conjugates capable of effective binding of both MTX and ASO moieties. Since click chemistry has been extensively used to covalently join two proximally bound molecules into one in template-directed synthesis [19], we chose this facile azide–alkyne 1,3-cycloaddition to accomplish RNA template-directed conjugation between MTX and bipartite ASO. This strategy required two synthetic precursor libraries: MTX analogs containing a linker-azide, and bipartite ASOs connected by a branched linker containing a terminal alkyne. Considering the variables mentioned above, a set of six MTX analogs and ten bipartite ASOs were designed as potential combinatorial building blocks for template-directed synthesis.

For MTX, we considered placing the linker-azide on the end of one of the two N-(2-aminoethyl)ethanolamine substituents, as we had previously shown that extending these substituents with an ethylamine was not only compatible with tau RNA hairpin binding and stabilization but increased potency in these respects [17]. We also considered adding the linker to MTX analogs MTX-3 and MTX-4, to the third or fourth N-(2-aminoethyl)ethanolamine substituent on the other side of the anthracene-dione ring system. In these cases, the MTX core structure might bind in its usual way according to the bound NMR structure [16], with intercalation of the aromatic ring system and binding of the two amino alcohol side chains to the major groove, while the linker-azide would be located on the other side of the double-helical RNA (i.e., the compound would be “threaded” through the RNA helix). Linker length was also varied, with an 8-atom and 17-atom ethylene glycol chain connected to the terminal azide. The six MTX-linker-azide analogs (**M1**–**M6**) are depicted in Fig. 2a.

For bipartite ASOs, we chose a peptide-nucleic acid (PNA) backbone (Fig 2b). Antisense PNA binds very strongly to complemen-

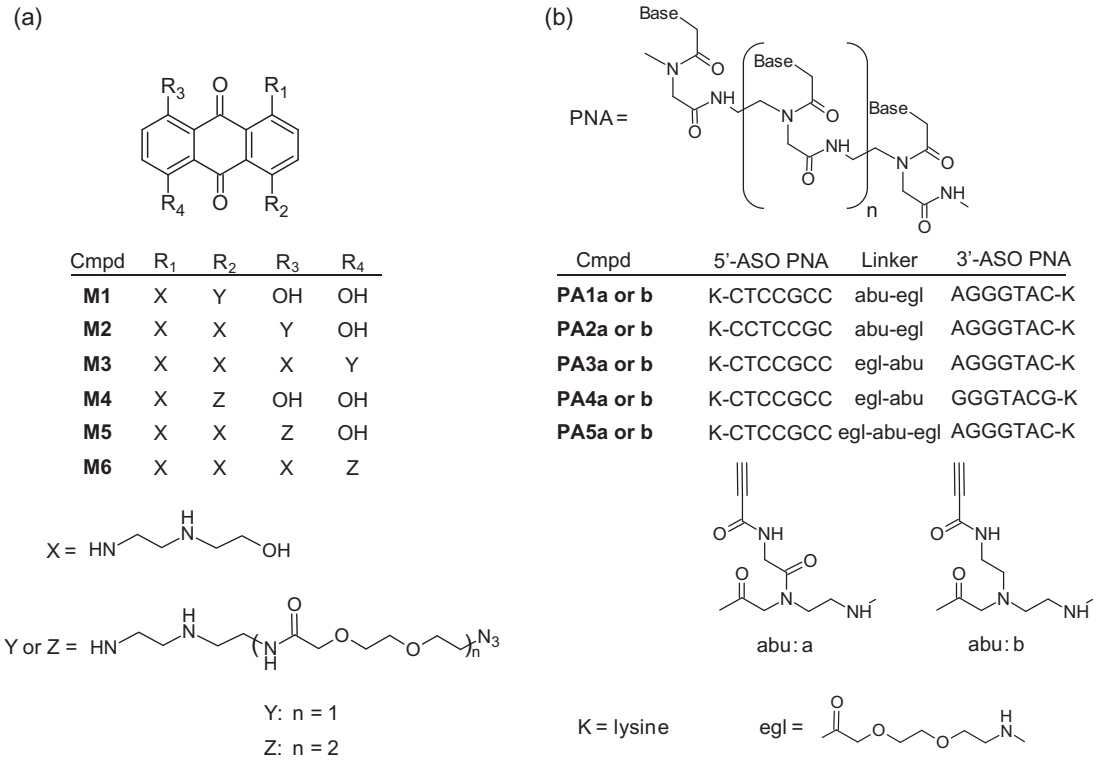

Fig. 2. (a) Target MTX-linker-azide analogs **M1**–**M6**. (b) Target bipartite PNA-linker-alkyne analogs **PA1**–**PA5** types a and b.

tary RNA, stronger than DNA or RNA ASOs do [20]. Moreover, we had previously synthesized bipartite PNA directed to the regions flanking the tau RNA hairpin and shown that these could bind better than the corresponding DNA or RNA ASOs: shorter sequences of bipartite PNA were required for effective binding [18]. We had found that seven nucleobases on either side of the linker provided strong binding to a synthetic 40-nucleotide RNA with the tau RNA hairpin and flanking sequences, and we therefore chose this PNA ASO as the starting point for the design of a set of ASOs for template-directed synthesis. Varying this bipartite PNA with one or two ethylene glycol (egl) units as the linker provided optimal binding to tau RNA, although a 3 × egl linker also allowed good binding [18].

In place of one of the egl units, we designed branched alkyne building units (ABUs) a and b (Fig. 2b). In the ABU, the alkyne tether was constructed onto N-(2-aminoethyl)glycine, the PNA backbone building block, connected by either an amide function (ABU a) or a tertiary amine (ABU b), as they represent two different charges and degrees of conformational flexibility. The terminal alkyne was directly connected to an electron-withdrawing amide group, which was reported to dramatically increase alkyne reactivity with azides, even in absence of Cu(I) catalyst [21]. With this alkyne design, the Hüisgen 1,3-cycloaddition will not occur when the reactants are at μM concentration at ambient temperature. However, in the presence of the RNA template, with MTX and PNA both bound, proximity between azide and alkyne should allow click chemistry to proceed and thereby conjugate MTX to the PNA. Along with the nature of the linker branching, several other variations in the bipartite PNA were explored. First ABUs were placed either to the left or to the right of an egl unit (Fig. 2b, **PA1** or **PA3**, respectively) or in the middle of two egl units (**PA5**). We also shifted the sequence of the PNA portion to which the ABU is directly attached by one nucleobase (**PA2** and **PA4**), in the event that base pairing immediately proximal to the ABU might interfere with the availability of the alkyne for the click reaction.

2.2. Template-directed synthesis

M1–**6** and types a and b of **PA1**–**5** were synthesized as described in supporting information. With the set of six MTX-linker-azides and ten bipartite PNA-linker alkynes, 6 × 10 RNA template-directed click reactions were carried out in parallel. We anticipated that only certain reactant combinations may accomplish azide–alkyne cycloaddition in the presence of synthetic 40-nucleotide tau RNA template. We performed the click reactions by incubating RNA oligonucleotide (10 μM), bipartite PNA alkyne (10 μM) and MTX azide (100 μM) in water at ambient temperature for four days. At the same time, 6 × 10 corresponding control reactions were tested in the absence of the RNA template. All 120 reactions were directly examined by MALDI-MS following incubation. As expected, little or no conjugate product peak was found in any of the control reactions (e.g. Fig. 3a). Only one template-directed reaction out of 60 (**M1** plus **PA5b**) clearly resulted in the corresponding conjugate product as identified by MALDI-MS (Fig. 3b). Thus, the RNA oligonucleotide representing the tau hairpin and flanking sequences could effectively serve as a template and facilitate the click reaction between **M1** and **PA5b**.

We also tested a synthetic RNA oligonucleotide comprised of 19 adenosides and 1 cytosine, which cannot generate any RNA secondary structure by itself in solution. A control experiment with this unstructured RNA, instead of the tau-based oligonucleotide, was performed under the same reaction conditions between **M1** azide and **PA5b** alkyne. Compared with the conjugate peak discovered in the combinatorial chemistry strategy, the product MS signal was very minor (not shown), similar to that seen with no RNA template (Fig. 3a), further validating that the RNA hairpin

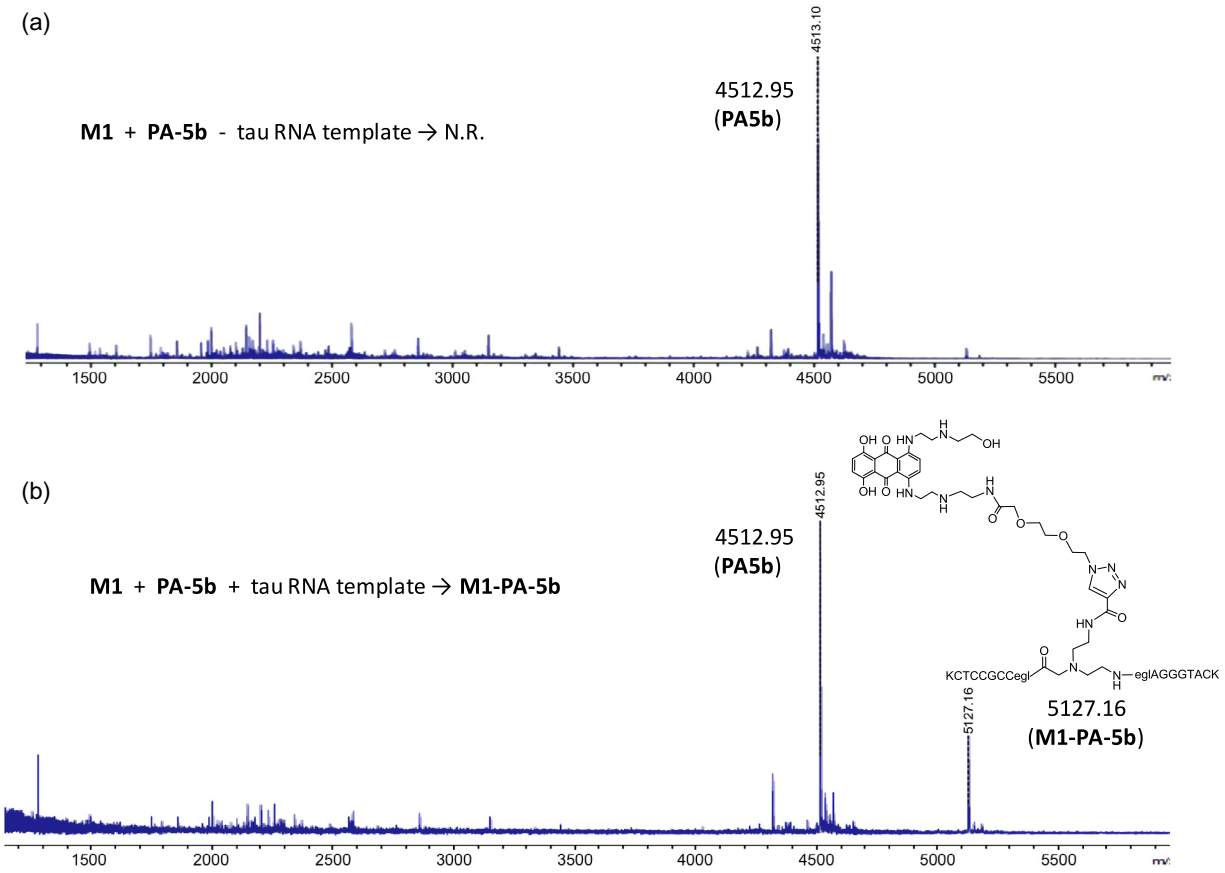

Fig. 3. MALDI-TOF mass spectrometry results from the reaction of **M1** with **PA5b** in the absence (a) or presence (b) of template tau RNA oligonucleotide.

and flanking sequences specifically promoted the formation of the MTX–PNA conjugate.

2.3. Biological results

The identity of the resulting click product **M1**–**PA5b** was confirmed by resynthesis by solid-phase on a larger scale, and this resynthesis also allowed biological evaluation. However, the MTX–PNA conjugate proved to be cytotoxic in several different cell lines, precluding analysis of effects on tau exon 10 splicing, either from a mini-gene construct or from endogenous tau pre-mRNA. Although the anticancer agent MTX is well known to be cytotoxic, our hope was that conjugation to PNA would attenuate this effect. While this was indeed the case (MTX cytotoxicity ~100 nM; **M1**–**PA5b** cytotoxicity ~1 μM), the reduced cytotoxicity of **M1**–**PA5b** was still insufficient for analysis of effects on splicing in cells, which appeared to be occurring at 1–3 μM. Installation of a cell-penetrating peptide (8 × lysine) on the C-terminus onto a closely similar conjugate (**M1**–**PA6**) did not improve potency toward splice inhibition enough to clearly separate this effect from cytotoxicity.

Despite the cytotoxicity problem, conjugate **M1**–**PA6** could still be tested for *in vitro* effects on tau exon 10 RNA splicing. We had

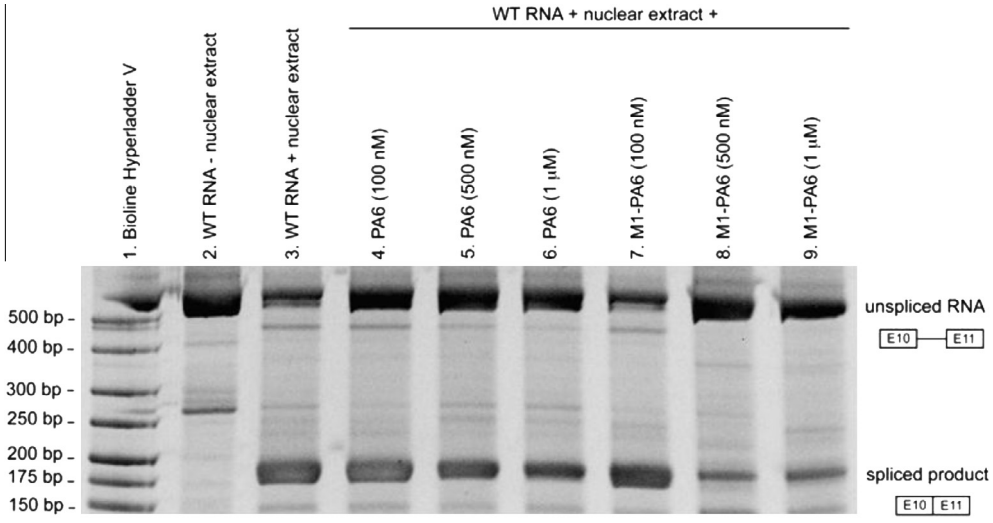

Fig. 4. Inhibition of tau exon 10 splicing by **PA6** or **M1**–**PA6** under cell-free conditions.

previously reported a system for cell-free splicing of tau exon 10 using nuclear extract from HeLa cells and an RNA splicing unit with exon 10, a shortened intron 10 and exon 11 [18]. **M1**–**PA6** could inhibit splicing of exon 10 to exon 11 in a concentration-dependent manner, with almost complete inhibition at 500 nM, whereas unconjugated bipartite PNA **PA6** alone was much less effective (Fig. 4). **MTX** alone showed little effect up to 1 μM (data not shown). Thus, the conjugation of **MTX** to **PA6** led to a clear increase in potency with respect to inhibition of tau exon 10 splicing compared with either unconjugated component alone.

3. Conclusions

We have successfully carried out what is to our knowledge the first template-directed synthesis targeting a structured RNA. We found that out of 60 possible PNA–MTX combinations, only one led to synthesis of a conjugate that was dependent on the presence of an RNA oligonucleotide representing the tau hairpin and flanking sequences. The successful specific template-directed conjugation strongly suggests that MTX and bipartite PNA portions simultaneously bind to the RNA to bring the reactive azide and alkyne into proximity and with proper alignment to allow 1,3-cycloaddition. While the PNA–MTX conjugate exhibited cytotoxicity that precluded proper evaluation of its effects on tau pre-mRNA splicing in cells, a cell-free splicing assay demonstrated that the conjugate is a much more effective inhibitor of tau exon 10 splicing than either bipartite PNA or MTX component are alone. Thus, these findings provide a proof of principle that compounds targeting an RNA structure and inhibiting a specific splicing event can be discovered through template-directed synthesis.

4. Experimental

The synthesis, purification and characterization of MTX analogs **M1**–**M5**, bipartite PNA analogs **PA1**–**PA5** (**a** and **b** for each), and **M1**–**PA5b** and **M1**–**PA6** are fully described in Appendix A (Supplementary materials).

4.1. RNA template-directed click cyclization and the control reactions

For each combination of MTX azide **M1** to **M6** and bipartite PNA alkyne **PA-1** to **PA5** (types a and b), a solution of the azide (100 μM), alkyne (10 μM) and synthetic RNA 5′GGGAGGCGGCAG UGUGAGUACCUUCACACGUCCCAUGCGC3′ (10 μM) in 50 μL H_2O was incubated at ambient temperature for 4 d. All reaction solutions were directly examined by MALDI-MS. Each of the corresponding 60 control reactions were carried out and analyzed in exactly the same way but in the absence of RNA template. Another control reaction was run with an unstructured RNA template: A solution of azide **M1** (100 μM), alkyne oligomer **PA**–**5b** (10 μM) and a synthetic RNA 5′AAAAAAAAAAAAAACAAAAA3′ (10 μM) in 50 μL H_2O incubated for 4 d. The reaction solution was directly examined by MALDI-MS.

4.2. HeLa cell nuclear extract preparation and in vitro splicing assay

Nuclear extracts were prepared from HeLa cells by a protocol adapted from Dignam et al. [22] The *In vitro* splicing assays were carried out as previously described [18]. Briefly, splicing reactions were performed for 3 h at 30 °C in reaction volumes of 25 μL. Reactions contained 10 μL HeLa nuclear extract, 4 μL buffer D (20 mM HEPES-KOH, pH 8.0, 100 mM KCl, 0.2 mM EDTA, 20% (v/v) glycerol, 0.5 mM PMSF, 1 mM DTT), 20 fmol splicing unit RNA, 0–1 μM test compound, 20 mM phosphocreatine, 0.5 mM ATP, 3.2 mM MgCl2, 40 mU/μL creatine phosphokinase, 2.6% v/v polyvinyl alcohol and 20 mM HEPES-KOH pH 7.3. In negative control reactions, HeLa nuclear extract was substituted with extra buffer D. RNA was isolated by phenol/chloroform precipitation and treated with DNase. Spliced products were amplified by reverse-transcription PCR with primers specific for the splicing unit RNA and detected by 20% acrylamide gel electrophoresis in TBE buffer with SYBR Gold staining under UV light.

Acknowledgments

This work was supported by Grant 20101211 from the Alzheimer Drug Discovery Foundation and Grant R21 NS079576 from the National Institutes of Health.

Appendix A. Supplementary material

Supplementary data associated with this article can be found, in the online version, at http://dx.doi.org/10.1016/j.bioorg.2014.03.001.

References

[1] A. Bugaut, S. Balasubramanian, Nucleic Acids Res. 40 (11) (2012) 4727–4741.
[2] A. Serganov, E. Nudler, Cell 152 (1–2) (2013) 17–24.
[3] C.J. McManus, B.R. Graveley, Curr. Opin. Genet. Dev. 21 (4) (2011) 373–379.
[4] F. Mignone, C. Gissi, S. Liuni, G. Pesole, Genome Biol. 3 (3) (2002). REVIEWS0004.
[5] J.R. Thomas, P.J. Hergenrother, Chem. Rev. 108 (4) (2008) 1171–1224.
[6] C.B. Carlson, O.M. Stephens, P.A. Beal, Biopolymers 70 (1) (2003) 86–102.
[7] L. Guan, M.D. Disney, ACS Chem. Biol. 7 (1) (2012) 73–86.
[8] V.M. Lee, M. Goedert, J.Q. Trojanowski, Annu. Rev. Neurosci. 24 (2001) 1121–1159.
[9] M. Hutton, C.L. Lendon, P. Rizzu, M. Baker, S. Froelich, H. Houlden, S. Pickering-Brown, S. Chakraverty, A. Isaacs, A. Grover, J. Hackett, J. Adamson, S. Lincoln, D. Dickson, P. Davies, R.C. Petersen, M. Stevens, E. de Graaff, E. Wauters, J. van Baren, M. Hillebrand, M. Joosse, J.M. Kwon, P. Nowotny, P. Heutink, et al., Nature 393 (6686) (1998) 702–705.
[10] M.S. Wolfe, J. Biol. Chem. 284 (10) (2009) 6021–6025.
[11] M.G. Spillantini, J.R. Murrell, M. Goedert, M.R. Farlow, A. Klug, B. Ghetti, Proc. Natl. Acad. Sci. USA 95 (13) (1998) 7737–7741.
[12] A. Grover, H. Houlden, M. Baker, J. Adamson, J. Lewis, G. Prihar, S. Pickering-Brown, K. Duff, M. Hutton, J. Biol. Chem. 274 (21) (1999) 15134–15143.
[13] L. Varani, M. Hasegawa, M.G. Spillantini, M.J. Smith, J.R. Murrell, B. Ghetti, A. Klug, M. Goedert, G. Varani, Proc. Natl. Acad. Sci. USA 96 (14) (1999) 8229–8234.
[14] C.P. Donahue, C. Muratore, J.Y. Wu, K.S. Kosik, M.S. Wolfe, J. Biol. Chem. 281 (33) (2006) 23302–23306.
[15] C.P. Donahue, J. Ni, E. Rozners, M.A. Glicksman, M.S. Wolfe, J. Biomol. Screen. 12 (6) (2007) 789–799.
[16] S. Zheng, Y. Chen, C.P. Donahue, M.S. Wolfe, G. Varani, Chem. Biol. 16 (5) (2009) 557–566.
[17] Y. Liu, E. Peacey, J. Dickson, C.P. Donahue, S. Zheng, G. Varani, M.S. Wolfe, J. Med. Chem. 52 (21) (2009) 6523–6526.
[18] E. Peacey, L. Rodriguez, Y. Liu, M.S. Wolfe, Nucleic Acids Res. 2012 (2012) 25.
[19] S.K. Mamidyala, M.G. Finn, Chem. Soc. Rev. 39 (4) (2010) 1252–1261.
[20] C.F. Bennett, E.E. Swayze, Annu. Rev. Pharmacol. Toxicol. 50 (2010) 259–293.
[21] A.T. Poulin-Kerstien, P.B. Dervan, J. Am. Chem. Soc. 125 (51) (2003) 15811–15821.
[22] J.D. Dignam, P.L. Martin, B.S. Shastry, R.G. Roeder, Methods Enzymol. 101 (1983) 582–598.